

Transpiration Cooling of Hypersonic Blunt Bodies with Finite Rate Surface Reactions

William D. Henline

(NASA-CR-177516) TRANSPIRATION COOLING OF
HYPERSONIC BLUNT BODIES WITH FINITE RATE
SURFACE REACTIONS (Sterling Federal
Systems) 35 p

CSSL 20D

N89-24580

Unclas

G3/34 0217938

CONTRACT NAS2-11555
February 1989



National Aeronautics and
Space Administration

Transpiration Cooling of Hypersonic Blunt Bodies with Finite Rate Surface Reactions

William D. Henline
Sterling Federal Systems, Inc.
1121 San Antonio Road
Palo Alto, CA 94303

Prepared for
Ames Research Center
CONTRACT NAS2-11555
February 1989



National Aeronautics and
Space Administration

Ames Research Center
Moffett Field, California 94035

TABLE OF CONTENTS

ABSTRACT	1
I. INTRODUCTION AND BACKGROUND.....	2
II. SCOPE OF WORK AND OBJECTIVES.....	3
III. DEVELOPMENT OF APPROXIMATE ANALYSIS	3
III.1 The General Two-Dimensional Multicomponent Reactive Boundary Layer Problem with Mass Addition at the Surface ...	4
III.1.1 Governing Equations	4
III.1.2 Transformation of Variables.....	7
III.2 Non-Similar Solutions and BLIMPK.....	9
III.3 Similarity Analysis and Solutions for Transpiration with Surface Reaction.....	10
IV. COMPARATIVE NEAR-STAGNATION SOLUTIONS FOR DIFFERENT GASEOUS INJECTANTS.....	14
V. DISCUSSION OF RESULTS AND EVALUATION OF SIMILARITY THEORY	17
VI. CONCLUSIONS AND RECOMMENDATIONS	18
VII. REFERENCES	19
FIGURES.....	20

PRECEDING PAGE BLANK NOT FILMED

LIST OF TABLES

- | | |
|--|----|
| 1. Flight Conditions for Maximum SSTO Ascent Heating | 19 |
|--|----|

LIST OF FIGURES

- | | |
|---|----|
| 1. SSTO surface temperature profiles showing effect of surface reactivity | 24 |
| 2. SSTO surface heat flux vs. wall mass injection; injection of pure N_2 | 25 |
| 3. SSTO surface heat flux vs. wall mass injection; injection of pure helium | 26 |
| 4. SSTO surface heat flux vs. wall mass injection; injection of pure argon | 27 |
| 5. SSTO surface heat flux vs. wall mass injection; comparison of fully catalytic results | 28 |
| 6. SSTO stagnation boundary layer species profiles; full-catalytic N_2 injection $\dot{m} = 0$. | 29 |
| 7. SSTO stagnation boundary layer species profiles; non-catalytic N_2 injection $\dot{m} = 0$. | 30 |
| 8. SSTO stagnation boundary layer species profiles; full-catalytic N_2 injection $\dot{m} = 0.30 \text{ lbm/ft}^2\text{-sec}$ | 31 |
| 9. SSTO stagnation boundary layer species profiles; non-catalytic N_2 injection $\dot{m} = 0.30 \text{ lbm/ft}^2\text{-sec}$ | 32 |

NOMENCLATURE

C	dimensionless parameter $\equiv (\rho\mu/\rho_e\mu_e)$
C_M^o	value of dimensionless mass transfer coefficient at zero mass injection rate
C_H^o	value of dimensionless heat transfer coefficient at zero mass injection rate
\bar{C}_p	species averaged specific heat, e.g. [=] BTU/lbm-deg R
C_{p_i}	specific heat for pure species i
c_t	constant relating thermal and mass diffusivity, (c.f. eq.(26) Ref.(9))
\bar{D}	reference binary diffusion coefficient(c.f. eq.(19) Ref.(9)) e.g. [=] ft^2/sec
T	thermal diffusivity for species i multi-component diffusion factor for species i (eq.(19) Ref.(9)) static gas enthalpy, e.g. [=] BTU/lbm static enthalpy for species i species averaged gas enthalpy enthalpy of surface material enthalpy of surface material removed by melting or erosion total enthalpy (static plus kinetic energy) diffusive mass flux of element k, e.g. [=] $lbm/ft^2\text{-sec}$ mass fraction of element k
M	molecular weight of gas mixture
M_i	molecular weight of species i
\dot{m}_e	mass removal rate of surface material by direct vaporization processes, e.g. [=] $lbm/ft^2\text{-sec}$
\dot{m}_g	mass injection gas rate from any in-depth pyrolysis process
$\dot{m}_{r,l}$	mass removal rate from surface by melting, etc.
P	total pressure, e.g. [=] atm.
\bar{Pr}	species averaged Prandtl number

q_c	diffusive heat flux, e.g. [=] BTU/ft ² -sec
q_{cond}	heat conducted internally to the heated surface
q_r	radiative heat flux to the body surface
R	universal gas constant
r	local streamline radius measured normal to the body symmetry axis, e.g. [=] ft
r_o	local body radius
\bar{S}_c	species averaged Schmidt number
T	local fluid temperature, e.g. [=] deg. R
u	boudary layer tangential velocity, e.g. [=] ft/sec
U_e	boundary layer edge tangential velocity
v	boundary layer normal velocity component
x_i	mole fraction of species i

Greek Symbols

α_{ki}	mass fraction of element k in species i
β_N	nose radius parameter (c.f. eq(23), Goulard Ref.(11))
λ	gas phase thermal conductivity, e.g. [=] BTU/ft-sec deg R
μ	gas phase viscosity, e.g. [=] lbm/ft-sec
ϕ_k	elemental reaction source term, e.g. [=] lbm/ft ³ -sec
ρ	gas phase density, e.g. [=] lbm/ft ³

Subscripts and Superscripts

e	boundary layer edge value
FC'	fully catalytic state
i	species i
k	elemental species k
NC'	non catalytic state
ν	local radius exponent, $\nu = 1$, for axisymmetric $\nu = 0$, for planar
w	body surface or "wall" value

ABSTRACT

Transpiration cooling of hypersonic aircraft and planetary entry vehicles has often been proposed to help reduce surface heating and maintain operating temperatures within the limits of available materials technology. For example, proposed aircraft which can take off horizontally and directly achieve orbital velocity (Single Stage to Orbit, (SSTO)) will experience very high heating rates under flight conditions of high enthalpy and high stagnation pressure. The dominant surface heating mechanism for these situations will be conduction and convection with relatively low levels of radiative heating. Transpiration cooling by mass addition can be quite effective in blocking such dissipative heat fluxes. This paper presents a quantitative study of the effect of transpiration cooling on a specific SSTO maximum heating case. The analysis is performed for the stagnation region of the vehicle using both similarity theory and a numerical, non-similar reactive boundary layer solution program, BLIMPK. An outline of both methods of analysis is presented, and comparisons are made between the determined heat fluxes. Additional results are presented for the effect of mass addition of pure nitrogen, helium and argon on heat flux and boundary layer species profiles. The effect of transpiration on the heat flux is examined for surfaces of different chemical reactivity. It is shown how the non-similar numerical, BLIMPK, results can be used to develop a heat transfer coefficient correlation in the presence of mass addition from the analytical heat flux expressions obtained from similarity theory. Suggestions are made for future research and experimental study.

I. INTRODUCTION AND BACKGROUND

Transpiration cooling by injection of fluids into hypersonic boundary layers has long been recognized as an effective means of mitigating the effects of conductive and convective heat fluxes on high speed re-entry vehicles. (Ref. 1,2,3) It is also a primary mechanism in blocking dissipative heat fluxes in ablative heat shield systems. As such, this active means of thermal protection will be most efficient in situations where the dominant surface heat flux is dissipative rather than radiative. Usually transpiration cooling would then be applicable for use on nose cones and flight (and control) surface leading edges of relatively small curvature typical of high L/D re-useable, re-entry vehicles. The flight regime of these applications will often pass through regions of maximum total heating at quite high stagnation pressures. As a result the dominant heating mechanism will be conduction and convection. This paper presents an analysis of the transport phenomena associated with transpiration into hypersonic boundary layers on generic blunt bodies of revolution (sphere-cones). Results will be presented for a specific trajectory maximum heating point of a hypersonic, Single Stage to Orbit (SSTO) vehicle. In the future, such aircraft are envisioned to take off horizontally from a runway and continuously thrust directly into orbit. As described by M. E. Tauber (Ref. 4) these flights will encounter maximum stagnation heating during the ascent phase, and this will be almost entirely dissipative in nature. Optimum design and determination of thermal protection materials requires knowledge of surface heat fluxes and temperatures. Transpiration cooling can dramatically affect these quantities, and this study will provide some quantitative estimates of the effects of operating parameters on surface heating for an SSTO ascent.

An additional phenomenon which can significantly affect heating in hypersonic flight is the reactivity of vehicle surface material. When atomic species from dissociated boundary layer gases reach the relatively cool surface of the vehicle, they can recombine and release their formation energy directly to the surface. The amount of energy released will depend on the inherent surface reactivity (or catalycity) and the rate of supply of atoms to the surface. Transpiration can most definitely impinge on the rate of atom supply, and this interaction will be examined.

II. SCOPE OF WORK AND OBJECTIVES

The objective of this study is to develop an approximate methodology capable of calculating the degree of transpiration cooling possible at various fluid injection rates near the stagnation region of high Mach Number external flows such as occur on SSTO type vehicles. Analytical solutions derived from similarity assumptions as well as solutions obtained from a numerical non-similar boundary layer computer code (BLIMPK) will be applied. Information obtained here will be useful in determining candidate thermal protection materials. Additional detailed information on the effect of mass injection rate and surface catalycity on boundary layer atomic species profiles will be examined and related to the effect of the transpiration cooling mechanism. Finally, surface heat flux expressions derived from similarity theory will be compared with the numerical, non-similar results. This will provide a limited check on the validity of the simplified method.

III. DEVELOPMENT OF APPROXIMATE ANALYSIS

The mathematical analysis of mass injection into reactive, hypersonic shock layers requires a fundamental approach, necessitated by the alteration of the surface boundary conditions. Basically the addition of mass at the boundary introduces an inhomogeneity which changes the shape of the boundary layer velocity, enthalpy and species concentration profiles. Even without this complication, a complete two or three dimensional solution of the thin shock or boundary layer governing equations requires complex numerical methods. It is, however, still important to ascertain if certain approximate methods will suffice to provide engineering estimates of surface heating.

Attempts at analytical description of mass injection into boundary layers began at least as early as 1951 with W. E. Stewart (Ref. 5) of M.I.T. He presented a similarity solution to the case of heat and mass transfer from the surface of a heated (or cooled) fixed temperature flat plate immersed in a boundary layer flow with mass addition at the surface. A constant property generalized solution was presented. This work will be alluded to later in this paper. In 1961 and somewhat later P. A. Libby and others (Ref. 6,7) obtained numerically augmented similarity solutions to the case of stagnation region transpiration cooling of hypersonic blunt bodies at

high mass injection rates. In 1959 P. M. Chung of NASA Ames Research Center (Ref. 8) supplied a partial similarity solution to stagnation region mass injection in the presence of finite rate surface reactions. J. T. Howe (Ref. 2) has given a synopsis of correlations, semi-analytical solutions, and numerical solutions for high Mach Number stagnation region mass addition problems (c.a. 1964). All of these approaches have in common the presumption of reactive thermo-chemical equilibrium among the boundary layer dissociation reactions as well as equilibrium at the shock or boundary layer edge. Many features of these previous attempts will be shared by the approximate methods and results presented in this paper.

III.1 THE GENERAL TWO-DIMENSIONAL, MULTICOMPONENT REACTIVE BOUNDARY LAYER PROBLEM WITH MASS ADDITION AT THE SURFACE

There are a very large number of authors to solutions of this general problem, and no attempt is made to refer to them in this study. Probably the most lucid and still perhaps the most accurate solution of the two-dimensional axisymmetric problem is the integral matrix method numerical solution of E. P. Bartlett and R. M. Kendall (Ref. 9 , 1965). This method, embodied in the computer code BLIMPK, has been adapted to the specific transpiration cooling problems examined here, and reacting boundary layer results from this code are given below. A brief description of the code and solution characteristics is also provided. At this point, however, the boundary layer governing equations of Bartlett and Kendall will be used as a basis set for the level of description desired in this study. These equations will also serve as a starting point for the more simplified analysis presented later.

III.1.1 GOVERNING EQUATIONS

In the continuum, hypersonic limit under the assumption that the shock and boundary layers are thin compared to the body dimension, the following conservation equations are applicable for a two-dimensional, axisymmetric blunt body. The coordinate system (s,y) is curvilinear and fixed to the body surface with origin at the stagnation point; (s) is the streamline variable, and (y) is the body normal variable.

Total Continuity:

$$\frac{1}{r_o^\nu} \frac{\partial(\rho u r^\nu)}{\partial s} + \frac{\partial(\rho v)}{\partial y} = 0. \quad (1)$$

Conservation of Species (i):

$$\rho u \frac{\partial \bar{K}_k}{\partial s} + \rho v \frac{\partial \bar{K}_k}{\partial y} = \frac{\partial}{\partial y} (j_k) + \phi_k \quad (2)$$

where,

$$j_k = \frac{\rho \bar{D} \mu_2}{\mu_1 \mathcal{M}} \left[\frac{\partial \bar{Z}_k}{\partial y} + (\bar{Z}_k - \bar{K}_k) \frac{\partial \ln \mu_2}{\partial y} \right] + \sum_i \alpha_{ki} D_i^T \frac{\partial \ln T}{\partial y} \quad (3)$$

Streamwise Momentum Conservation:

$$\rho u \frac{\partial u}{\partial s} + \rho v \frac{\partial u}{\partial y} = \frac{\partial}{\partial y} \left(\mu \frac{\partial u}{\partial y} \right) - \frac{\partial P}{\partial s}. \quad (4)$$

Body Normal Momentum Conservation:

$$\frac{\rho u^2}{r_o} = \frac{\partial P}{\partial y}. \quad (5)$$

Conservation of Total Energy:

$$\rho u \frac{\partial H_T}{\partial s} + \rho v \frac{\partial H_T}{\partial y} = \frac{\partial}{\partial y} (q_c + q_r), \quad (6)$$

where,

$$q_c = \mu \frac{\partial (u^2)}{\partial y} + \lambda \frac{\partial T}{\partial y} + \frac{\rho \bar{D} \mu_2}{\mu_2 \mathcal{M}} (Q_s) \quad (7)$$

where,

$$Q_s = \frac{\partial \bar{h}}{\partial y} - \left(\bar{C}_p + \frac{C_i^2 R}{\mu_1 \mu_2} \right) \frac{\partial T}{\partial y} + C_i R T \frac{\partial \mu_3}{\partial y} + (\bar{h} - h + C_i R T \mu_3) \frac{\partial \mu_2}{\partial y} \quad (8)$$

These equations are to be supplemented by mechanical and caloric equations of state as well as the appropriate boundary conditions. Specifically, H_T is the total enthalpy (static plus kinetic)

$$H_T = h + \frac{u^2}{2} \quad (9)$$

$$h = \sum_i K_i h_i \quad (10)$$

$$h_i = \int_0^T C_{p_i} dT + h_i^o \quad (11)$$

$$\bar{C}_p = \sum_i K_i C_{p_i} \quad (12)$$

$$\bar{K}_k = \sum_i \alpha_{ki} K_i \quad (13)$$

$$\bar{Z}_k = \sum_i \alpha_{ki} Z_i \quad (14)$$

$$Z_i = \mathcal{M}_i x_i / F_i \mu_2 \quad (15)$$

$$\mu_1 = \sum_i x_i F_i \quad (16)$$

$$\mu_2 = \sum_i \frac{\mathcal{M}_i x_i}{F_i} \quad (17)$$

$$\mu_3 = \sum_i \frac{Z_i}{\mathcal{M}_i} \quad (18)$$

$$(19)$$

The simplest boundary conditions in effect here are the following;

$$u(s, 0) = 0 \quad (20)$$

$$\rho(s, 0)v(s, 0) = \rho_w v_w \quad (21)$$

$$h(s, 0) = h_w \quad (22)$$

$$\bar{K}_k(s, 0) = \bar{K}_{kw} \quad (23)$$

Equations (22) and (23) could alternatively be replaced by wall diffusive flux balances.

III.1.2 TRANSFORMATION OF VARIABLES.

The above partial differential governing equations are, in general, non-linear and parabolic in form. A hypersonic blunt body has a sub-sonic flow region in the vicinity of the stagnation point, and an iterative problem must be solved if the proper boundary conditions are to be imposed on the above equations. In thin shock layer and boundary layer problems, this is usually accomplished in an approximate manner. Inviscid shock layer governing equations can be solved to provide an approximation of the body surface pressure distribution. With this as a fixed boundary condition the boundary layer system is amenable to various numerical and semi-analytic solution techniques. In taking this approach here, the BLIMPK computer simulations with surface mass addition represent the parabolic numerical solutions, while similarity analysis will be used to obtain simpler analytic results. In either method, the first step is to reduce the order of term by term and variable coupling effects through the use of variable transformations. The transformation of variables will group dominant effects into specific terms. In axisymmetric boundary layer theory the Levy-Lees transformations are the most useful. These are;

$$\xi = \int_0^s \rho_e U_e \mu_e r_o^{2\nu} ds \quad (24)$$

$$\eta = \frac{r_o^\nu U_e}{\sqrt{2\xi}} \int_0^\nu \rho dy \quad (25)$$

and

$$f = f_w + \int_0^\eta \frac{u}{U_e} d\eta \quad (26)$$

is the stream function. Omitting algebraic details for clarity, (see Ref. 9) the boundary layer equations transform over to the following;

Continuity:

$$\rho v = -\frac{\rho_e U_e \mu_e r_o^\nu}{\sqrt{2\xi}} \left[f + (2\xi) \frac{\partial f}{\partial \xi} \right] - \frac{f'}{r_o^\nu} \sqrt{2\xi} \frac{\partial \eta}{\partial s} \quad (27)$$

Species (i) Conservation:

$$f\tilde{K}'_k + [-j_k]' + \phi_k = 2 \left(f' \frac{\partial \tilde{K}_k}{\partial \ln \xi} - \tilde{K}'_k \frac{\partial f}{\partial \ln \xi} \right) \quad (28)$$

ξ Momentum:

$$ff'' + [Cf''']' - \frac{2\xi}{\rho U_e^2} \{P'\} - \beta f'^2 = 2 \left(f' \frac{\partial f'}{\partial \ln \xi} - f'' \frac{\partial f}{\partial \ln \xi} \right) \quad (29)$$

$$P' = \frac{\partial P}{\partial \xi} + P' \left[\frac{\partial}{\partial \xi} \left(\frac{r_o^\nu U_e}{\sqrt{2\xi}} \int_o^\nu \rho dy \right) \right] \quad (30)$$

η Momentum:

$$P' = \frac{U_e \sqrt{2\xi}}{r_o^{\nu+1}} (f')^2 \quad (31)$$

Energy Conservation:

$$fH'_T + [-q_c + q_r]' = 2 \left(f' \frac{\partial H_T}{\partial \ln \xi} - H'_T \frac{\partial f}{\partial \ln \xi} \right) \quad (32)$$

The individual diffusive fluxes annotated in the above equations take the form;

$$j_k = - \frac{\rho_e U_e \mu_e r_o^\nu}{\sqrt{2\xi}} \left(\frac{C}{\bar{S}_c} \right) \left[\tilde{Z}'_k + (\tilde{Z}_k - \tilde{K}_k) \mu'_4 \right] \quad (33)$$

$$\mu_4 = \ln(\mu_2 T^{c_1}) \quad (34)$$

and,

$$q_c = - \frac{\rho U_e \mu_e r_o^\nu}{\sqrt{2\xi}} C' \left[f' f'' U_e^2 + \frac{\bar{C} p}{Pr} T' + \mathcal{H}' \right]. \quad (35)$$

$$\mathcal{H}' = \frac{1}{\bar{S}_c} \left[\tilde{h}' - \left(\bar{C} p + \frac{c_1^2 R}{\mu_1 \mu_2} \right) T' + c_1 R T \mu'_3 + (\tilde{h} - h + c_1 R T \mu_3) \mu'_4 \right] \quad (36)$$

The boundary conditions for the transformed system can take on a variety of different acceptable values, but the following are most typical.

$$f'_{edge} = \frac{u}{U_e}|_{edge} \quad (37)$$

$$f''_{edge} = f' \frac{d}{df} (u/U_e)|_{edge} \quad (38)$$

$$H_T|_{edge} = H_T(actual)|_{edge} \quad (39)$$

$$H'_T|_{edge} = 0 \quad (40)$$

$$\tilde{K}_k|_{edge} = \tilde{K}_k|_{edge}(actual), \quad (41)$$

$$\tilde{K}'_k|_{edge} = 0 \quad (42)$$

$$f(\xi, 0) = f_w \quad (43)$$

$$H_T(\xi, 0) = H_{Tw} \quad (44)$$

$$\tilde{K}_k(\xi, 0) = \tilde{K}_{kw} \quad (45)$$

H_{Tw} and \tilde{K}_{kw} can also be indirectly determined by the following surface mass and energy balances. Whether these are fixed values or subject to the constraint equations depends on the actual physical nature of the surface boundary.

$$\dot{m}_g h_g + \dot{m}_c h_c - \sum_l \dot{m}_{rl} h_l - (\rho_w v_w) h_w - q_{cw} + q_{rw} - q_{cond} = 0, \quad (46)$$

$$\dot{m}_g \tilde{K}_{kg} + \dot{m}_c \tilde{K}_{kc} - \sum_l \dot{m}_{rl} \tilde{K}_{kl} - (\rho_w v_w) \tilde{K}_{kw} - j_{kw} = 0. \quad (47)$$

III.2 NON-SIMILAR SOLUTIONS AND BLIMPK

The terms on the right hand sides of the transformed governing equations and associated terms in the dissipative fluxes are known as non-similar terms and can be significant in situations where either the surface or boundary layer edge conditions have large variations along the streamwise direction. This can happen with abrupt changes in body geometry, sudden changes in surface conditions such as abrupt changes in mass addition rates or surface reactivity, or rapid changes in edge conditions due to external flow effects.

Non-similar effects can only be evaluated by solving the complete set of governing equations. The current version of BLIMPK has been adapted

to numerically solve for the general case of mass addition and surface finite rate chemistry. BLIMPK uses an integral matrix procedure augmented with Newton-Raphson methods to numerically solve the non-similar boundary layer equations. In this study, solutions are obtained for the injection of pure nitrogen, helium and argon in the stagnation region of an SSTO vehicle. The surface of the vehicle is considered to be adiabatic and at a temperature corresponding to a surface energy balance where all incoming conductive and chemical energy is fully re-radiated to the vacuum. Fluid mass injection rates can be specified independently at any streamwise body station, and surface temperatures, species mass fractions and fluxes can be calculated. Plots of these quantities are shown and described in Section IV.

III.3 SIMILARITY ANALYSIS AND SOLUTIONS FOR TRANSPIRATION WITH SURFACE REACTION

A great many situations in hypersonics either do not exhibit non-similar behavior or these effects can be considered to be second order. In the vicinity of the stagnation point of blunt bodies, the boundary layer will be essentially similar in the streamwise direction. The calculation of surface temperatures and dissipative fluxes in this region is important in an engineering sense, since the stagnation region usually experiences the most severe combined heating in most flight situations. It will be useful to obtain approximate analytical expressions for these quantities and compare them with the more general non-similar results from BLIMPK.

To obtain a simplified solution it is assumed that all terms containing explicit dependency on the streamwise variable, ξ , are small and can be dropped. The more general boundary layer model outlined in Section III.1 includes the effects of both finite rate, homogeneous gas dissociation reactions as well as kinetic surface catalyzed re-combination reactions. Non-equilibrium kinetics effects are very non-linear and must be handled numerically. A great many cases of hypersonic blunt body flow will have high enough shock layer pressures to allow the dissociation reactions to reach thermochemical equilibrium by the time the flow reaches a boundary layer edge. This would be especially true in the subsonic region. Starting from an equilibrium edge, driving forces for displacement from chemical equilibrium are almost non-existent within the boundary layer, except near the surface where catalysis can be taking place. Under these conditions the reaction

source terms can also be eliminated from the governing equations. This assumption is almost universal in the similarity treatment of mass addition problems. Including these caveats, a set of similar boundary layer equations can now be derived. For this situation where the total shock layer thickness is considered very thin, the body normal momentum equation will be dropped, (i.e. $P' = 0$). The transformed similar boundary layer equations now become,

Total Continuity:

$$\rho v = -\frac{\rho_e U_e \mu_e r_o^\nu}{\sqrt{2\xi}} f \quad (48)$$

Conservation of k-th Elemental Species:

$$\frac{\bar{S}c}{C} \left[f - \left(\frac{C}{\bar{S}c} \right)' \right] \bar{K}_k' + \bar{K}_k'' = 0. \quad (49)$$

Streamwise, ξ , Momentum:

$$(f - C') f''' = \beta \left(f'^2 - \frac{\rho_e}{\rho} \right) \quad (50)$$

Energy:

$$\frac{\bar{P}r}{C'} \left[f - \left(\frac{C}{\bar{P}r} \right)' \right] H_T' + H_T'' = C' \left(\frac{1}{\bar{P}r} - 1 \right) U_e^2 f' f'' \quad (51)$$

Boundary Conditions will now take the form;

$$f(0) = f_w, \quad f'(0) = 0, \quad f'(\infty) = 1 \quad (52)$$

$$H_T(0) = H_w, \quad H_T(\infty) = H_T^e \quad (53)$$

$$\bar{K}_k(0) = \bar{K}_k^w, \quad \bar{K}_k(\infty) = \bar{K}_k^e. \quad (54)$$

The right hand sides of the momentum and energy equations still contain inhomogeneities associated with coupling of conduction, viscous dissipation and compression effects. As Lees (Ref.10) has pointed out, these terms are second order also for most hypersonic flows, since $Pr \approx 1$ and $f'^2 - \rho_e/\rho \approx 0$

when $T_w \ll T_e$. These assumptions are usually referred to as the "Cold Wall" approximation. With this premise then, a closed form solution is possible. W. E. Stewart (Ref.5) has previously obtained this solution in the form,

$$\Lambda(\xi, \eta) = \begin{cases} H_T^* = (H_T - H_T^w) / (H_T^e - H_T^w) \\ \bar{K}_k^* = (\bar{K}_k - \bar{K}_k^w) / (\bar{K}_k^e - \bar{K}_k^w) \end{cases} \quad (55)$$

satisfying the generic governing equation,

$$\frac{\Omega}{C} \left[f - \left(\frac{C}{\Omega} \right) \right] \Lambda' + \Lambda'' = 0, \quad (56)$$

where,

$$\Lambda(0, \Omega, -f_w) = 0 \quad (57)$$

$$\Lambda(\infty, \Omega, -f_w) = 1 \quad (58)$$

and,

$$\Omega = \begin{Bmatrix} 1.0 \\ \bar{S}_c \\ \bar{P}_r \end{Bmatrix} \quad (59)$$

Formally the solution is,

$$\Lambda(\eta, \Omega, -f_w) = \frac{\int_0^\eta \exp \left(- \int_0^\eta \frac{\Omega}{C} \left(f - \left(\frac{C}{\Omega} \right)' \right) d\eta \right) d\eta}{\int_0^\infty \exp \left(- \int_0^\eta \frac{\Omega}{C} \left(f - \left(\frac{C}{\Omega} \right)' \right) d\eta \right) d\eta} \quad (60)$$

with

$$\Lambda'(0, \Omega, -f_w) = \left\{ \int_0^\infty \exp \left(- \int_0^\eta \frac{\Omega}{C} \left(f - \left(\frac{C}{\Omega} \right)' \right) d\eta \right) d\eta \right\}^{-1} \quad (61)$$

Using this kind of analysis it is desired to obtain the total heat flux to the surface of the body in terms of the solution variables. This can be written as,

$$q_w^T = q_w + \sum_k j_k^w h_k(T_w) \quad (62)$$

where,

$$j_k^w = \rho_e U_e C_M (\bar{K}_k^w - \bar{K}_k^e) \quad (63)$$

$$C_M = C_w \left\{ \sqrt{\frac{\rho_e U_e}{2}} \gamma_e \left(\frac{\rho_e U_e \mu_e}{2\xi} \right)^{1/2} \right\} (\bar{S}c^w)^{-1} \bar{K}_k^{w*'}(0, \bar{S}c^w, -f_w) \quad (64)$$

$$q_w = \rho_e U_e C_H (H_T^w - H_T^e) \quad (65)$$

and

$$C_H = C_M \left(\frac{\bar{S}c^w}{\bar{P}r^w} \right) \frac{H_T^{w'}(0, \bar{P}r^w, -f_w)}{\bar{K}_k^{w*'}(0, \bar{S}c^w, -f_w)} \quad (66)$$

After performing the appropriate algebra, the following explicit expression for q_w^T can be obtained.

$$Q_w^* = (C_H/C_H^o) \mathcal{H}_T^* + \sum_k \frac{(C_M/C_H^o)}{\Psi_{rxn}^w} \left[\frac{\gamma_k^w k_k^w}{\rho_w v_w} (\bar{K}_k^e - \bar{K}_k^{EQ}) + (\bar{K}_k^I - \bar{K}_k^e) \right] \mathcal{H}_k^{w*} \quad (67)$$

where,

$$\Psi_{rxn}^w = 1 - \frac{\rho_e U_e C_M}{\rho_w v_w} - \frac{\gamma_k^w k_k^w}{\rho_w v_w} \quad (68)$$

$$\mathcal{H}_T^* = \frac{(H_T^w - H_T^e)}{(H_T^w(FC) - H_T^e)} \quad (69)$$

$$\mathcal{H}_k^{w*} = \frac{h_k^w}{(H_T^w(FC) - H_T^e)} \quad (70)$$

$$Q_w^* = \frac{(-q_w^T)}{\rho_e U_e C_H^o (H_T^e - H_T^w(FC))} \quad (71)$$

Two mathematical limits of this equation are of interest. These refer to the cases of either fully reactive (catalytic) or completely non-reactive wall reactions. Thus, for a fully catalytic wall $k_k^w \rightarrow \infty$, for all k ,

$$Q_w^*(FC) = (C_H/C_H^o) + \sum_k (C_M/C_H^o) (\bar{K}_k^e - \bar{K}_k^{EQ}) \mathcal{H}_k^{w*}(FC) \quad (72)$$

and for a non-catalytic wall, $k_k^w \rightarrow 0$,

$$Q_w^*(NC) = \mathcal{N}_H \mathcal{H}_T^*(NC) + \frac{\dot{m}_w^*}{(\dot{m}_w^* - \mathcal{N}_M)} \sum_k \frac{C_M}{C_H^o} (\bar{K}_k^e - \bar{K}_k^I) \mathcal{H}_k^{w*}(NC) \quad (73)$$

where,

$$\dot{m}_w^* = \frac{\rho_w v_w}{\rho_e U_e C_M^o} \quad (74)$$

$$\mathcal{N}_H = C_H / C_H^o \quad (75)$$

$$\mathcal{N}_M = C_M / C_M^o. \quad (76)$$

Goulard (Ref.11) has obtained the additional special limiting case for a cold wall, stagnation point value for C_H^o .

$$\lim_{\epsilon, f_w \rightarrow 0} \rho_e U_e C_H = \left(\frac{\rho_w \mu_w}{\rho_e \mu_e} \right) \sqrt{2 \rho_e \mu_e \beta_N (\bar{P} r^w)^{-1} \left[0.47 (\bar{P} r^w)^{1/3} \right]}. \quad (77)$$

Equations (67), (72) and (73) have a well recognized behavior as a function of \dot{m}_w^* . \mathcal{N}_H and \mathcal{N}_M are exponentially decreasing in \dot{m}_w^* (see Section V), and this leads to the general behavior as all previously published plots for mass addition with a fully catalytic wall. It shows the classic form of the blowing correction function for ablation and transpiration. However, the intermediate and non-catalytic cases exhibit a peak at lower values of mass injection. This non-classical behavior is due to addition of the injected gas enthalpy, which will be greater than the dissipative energy blocked by injection at low injection rates. This will occur, most probably, only in those situations where the injected gas equilibrates rapidly with the boundary layer. If there is a significant cold gas layer heat transfer resistance, then the added gas enthalpy will be less, and the maximum will be less or non-existent. An added feature of this maximal behavior displayed at low catalycity is the singular behavior of Equation (73). The maximum must occur when $\dot{m}_w^* = \mathcal{N}_M$. For the heat flux to remain finite at this point, $\sum_k j_k h_k$, in other words, the mass diffusive heat flux must become zero. This will be the balance point between heat flux due to mass diffusion and injected mass flux. This is consistent with intuition.

IV. COMPARATIVE NEAR-STAGNATION SOLUTIONS FOR DIFFERENT GASEOUS INJECTANTS

In addition to formal theoretical development, an objective of this study is the determination of quantitative transpiration cooling effects from stagnation region gas injection for a specific hypersonic flight case. Using the

non-similar numerical simulation, BLIMPK, a series of calculations were performed to compare the relative effectiveness of different molecular weight gases for stagnation cooling of an SSTO during maximum heating. As mentioned above, in hypersonic cruise, the maximum heating point will occur during ascent to orbit. Flight conditions typical of this are shown in Table 1. (Ref. 4) BLIMPK solutions were obtained for a range of stagnation point injection mass fluxes using nitrogen, helium and argon as coolant gases. An additional parameter in these calculations was the surface reactivity. Resultant heat fluxes correspond to a fully adiabatic vehicle wall with all energy ultimately being re-radiated to the vacuum. The effect of surface reactivity can be seen from the results for an equilibrium edge calculation for this small radius (1.5 inch) blunt nosed cone configuration. A plot of surface temperature and streamline coordinate is shown in Figure 1 . Curves are given for a relatively non-catalytic silica tile material coated with borosilicate glass, and for a case where the surface reactivity was increased 56-fold at a distance 2.5 inches from the stagnation point. The additional chemical energy available from a catalytic surface is significant, and in this SSTO case the stagnation heating is severe; even for a non-catalytic surface. Stagnation wall temperatures as high as 5000 deg F are not feasible for state-of-the-art high temperature materials. One hope of transpiration cooling is to bring these high surface temperatures down to within the safe operating range of existing materials.

Table 1

Flight Conditions for Maximum SSTO Ascent Heating

Freestream Conditions:	Stagnation Conditions:
Pressure: 1.1091×10^{-3} atm.	0.924 atm.
Density: 9.0475×10^{-5} lbm/ft ³	
Velocity: 26,380 ft/sec	
Altitude: 155,000 ft.	
Enthalpy:	13,899 BTU/lbm.

As mentioned above, a comparison study of different molecular weight gases as injectants was performed using BLIMPK. Figure 2 shows a plot of stagnation heat flux vs nitrogen injection rate for the sharp nose cone portion of the SSTO at maximum heating. This plot is dimensional to give an intuitive feel of the magnitude of required injected gas. For this flight condition, the freestream mass flux, $\rho_{\infty} v_{\infty}$, is approximately 1 lbm/ft²-sec; therefore, the injection rates are effectively dimensionless relative to the freestream. With reference to Figure 2 it is seen there exists the same form of functional behavior as the similarity solutions embodied in equations (67), (72) and (73). It is encouraging then, that for constant mass injection rates into laminar boundary layers, BLIMPK could be used to provide a semi-analytical correlation of the heat and mass transfer coefficient expressions and the parameters contained therein. Figures 3 and 4 show plots of stagnation transpiration cooled heat fluxes for helium and argon injection respectively. The relative influence of molecular weight is dramatic and in favor of lower weight species such as helium and hydrogen. This is further shown in Figure 5 where the fully catalytic results are shown on a common plot. Also shown here are the interpreted results of Chung (Ref. 8), which occur as straight lines for his fully catalytic and non-catalytic cases. The linear behavior is due to maintenance of a constant value of the function, ($\Psi_{rxn}^w = 0$ and 1.0) for variable injection rate. This, of course, is not occurring for the plots derived in this study, but the trend is the same. Energy release to the surface by catalytic recombination is important, and the effect of mass injection on this is discernable from the calculations in this study. The derived functionalities of total heat flux vs mass injection rate as well as the BLIMPK calculations show a diminishing return for the non-catalytic surface at higher and higher injection rates. An examination of the competing phenomena at the surface will shed some light on why this occurs. Figures 6 and 7 are BLIMPK results for species mass fraction profiles across the boundary layer at the stagnation point, respectively for a fully catalytic and non-catalytic surface. These results are for a zero mass injection rate and show that the boundary layer (with equilibrium edge) is essentially frozen at equilibrium except for the elemental nitrogen for the fully catalytic surface. It is also noted that the surface catalyzed gas phase dissociation reaction kinetic model considered here, oxygen total surface recombination is much less active than nitrogen. This is consistent

with the higher activation energy for nitrogen dissociation. Figures 8 and 9 show the same BLIMPK results for the very high rate of nitrogen injection of 0.30 lbm/ft²-sec. The large mass addition of nitrogen at the surface has flattened out the species profiles at the surface, and all profiles appear as almost identical. In the non-catalytic case, even though the elemental nitrogen no longer reacts at the surface, it is replaced at the surface by the injection of molecular nitrogen. As a result the overall effect is nearly the same as for a fully catalytic surface at these same high injection rates.

V. DISCUSSION OF RESULTS AND EVALUATION OF SIMILARITY THEORY

The functional results from similarity theory and BLIMPK discussed above are interesting and useful for estimating the order of magnitude of transpiration cooling needed to bring surface operating temperatures to within the operating limits of materials used for the thermal protection of hypersonic vehicles. Such estimates, at this point, can be considered only as order-of-magnitude in quality. Limitations which must be imposed include the existence of turbulence and shock layer interaction with injected gas. Injection of high mass fluxes in the stagnation region is known to trip turbulence at very low Reynolds numbers, resulting in fully developed turbulence just immediately off the stagnation point. If this occurs, the above estimates of surface heat flux as a function of mass rate of injection will be too optimistic. There is very little knowledge of the transition levels for this type of boundary layer flow. When injection rates get even higher than those resulting in turbulence, interaction with the bow shock will occur. The degree of shock displacement, or even the character or existence of a well defined shock will be in question. An entirely more general analysis would then be required to calculate heat fluxes.

Recalling that Figure 2 and equations (67), (72) and (73) indicate a good correspondence between similarity theory and the more general non-similar BLIMPK results near the stagnation point, it is possible to use the numerical data from the non-similar model to calculate specific correlational forms for the flux expressions obtained in similarity theory. If, as is plausible for most cases, it is assumed that $C_M/C_H \equiv 1.0$, then equation (67) contains only two adjustable parameters or functions. These are,

$$\mathcal{N}_H = C_H/C_H^o \quad (78)$$

and,

$$\mathcal{N}_M = C_M / C_M^o. \quad (79)$$

Many previous studies have, e.g. Ref.(12), have shown that the typical functionality for \mathcal{N} can be represented as,

$$\mathcal{N} = \frac{\kappa \dot{m}_w^*}{(e^{\kappa \dot{m}_w^*} - 1)}, \quad (80)$$

where, κ can be considered an adjustable constant. κ is usually of the order of unity, Ref.(12). This functional form is responsible for the classic exponentially decaying behavior for the surface conductive heat flux as a function of injected mass flux. This empirical form can then be used in place of the BLIMPK calculations where it can be assumed that the boundary layer maintains a self-similar or constant pattern form over the flight body.

VI. CONCLUSIONS AND RECOMMENDATIONS.

In flight situations where the freestream enthalpy and stagnation pressures are relatively high, the dominant surface heat flux will be due to conductive/ convective (dissipative) mechanisms. Transpiration cooling appears to offer an effective means of blocking this energy flux in the same manner as occurs in ablating systems. It is observed in this study that the beneficial effect of a non-catalytic surface becomes negligible at high mass injection rates. At these high mass rates, net surface heat transfer will be quite low, however. The absolute value of required injection rate for nearly complete heat blockage is uncertain due to a lack of detailed knowledge of transpiration on boundary layer turbulence and shock interference. It does appear that, for stagnation region heat transfer, similarity theory is an adequate description of mass addition in the presence of finite rate surface reactions.

Future studies should include definitive experiments to ascertain the injection rates required to trip turbulence for a variety of body shapes and flight conditions. Numerical computational studies should also be performed to examine the interaction between injected gas and the bow shock at very high injection rates. The threshold for this phenomena should also be investigated experimentally in an arc-jet environment. All of these experiments should range over enough conditions to be comparable to the above calculations and any future results.

VII. REFERENCES

1. Low, G.M., "The Compressible Laminar Boundary Layer with Fluid Injection," NACA TN-3404, March, 1955.
2. Howe, J.T. and Y.S. Sheaffer, "Mass Addition in the Stagnation Region for Velocity up to 50,000 Feet Per Second," NASA TR-R207, Aug., 1964.
3. Pappas, C.C. and A.F. Okuno, "Heat Transfer Measurement for Binary Gas Laminar Boundary Layers with High Rates of Injection," NASA TN D-2473, September, 1964.
4. Tauber, M.E., Menees, G.P., and H.G. Adelman, "Aerothermodynamics of Transatmospheric Vehicles," AIAA Paper 86-1257, Boston, Mass., June, 1986.
5. Stewart, W. E., Sc.D. Thesis, Massachusetts Institute of Technology, 1951.
6. Libby, P. A., "The Homogeneous Boundary Layer at an Axisymmetric Stagnation Point with Large Rates of Injection," Journal of the Aerospace Sciences, Jan., 1962, pp.48-60.
7. Fox, H. and P. A. Libby, "Helium Injection Into the Boundary Layer at an Axisymmetric Stagnation Point," Journal of the Aerospace Sciences, August, 1962, pp.926-933.
8. Chung, P. M., "Shielding Stagnation Surfaces of Finite Catalytic Activity by Air Injection in Hypersonic Flight," NASA TN D-27, August, 1959.
9. Bartlett, E. P. and R. M. Kendall, "An Analysis of the Coupled Chemically Reacting Boundary Layer and Charring Ablator," Part III, NASA CR-1062, August, 1965.
10. Lees, L., "Laminar Heat Transfer over Blunt Nosed Bodies at Hypersonic Speeds," Jet Propulsion, vol. 26, April, 1956, pp.259-269.
11. Goulard, R., "On Catalytic Recombination Rates in Hypersonic Stagnation Heat Transfer," Jet Propulsion, November, 1958, pp.737-745.
12. Moyer, C. B. and R. A. Rindal, "An Analysis of the Coupled Chemically Reacting Boundary Layer and Charring Ablator," Part II, NASA CR-1061, 1968.

Figure 1

SSTO Surface Temperature Profiles
showing effect of surface reactivity

□ = Silica Tiles

○ = 56-fold increase in surface reactivity

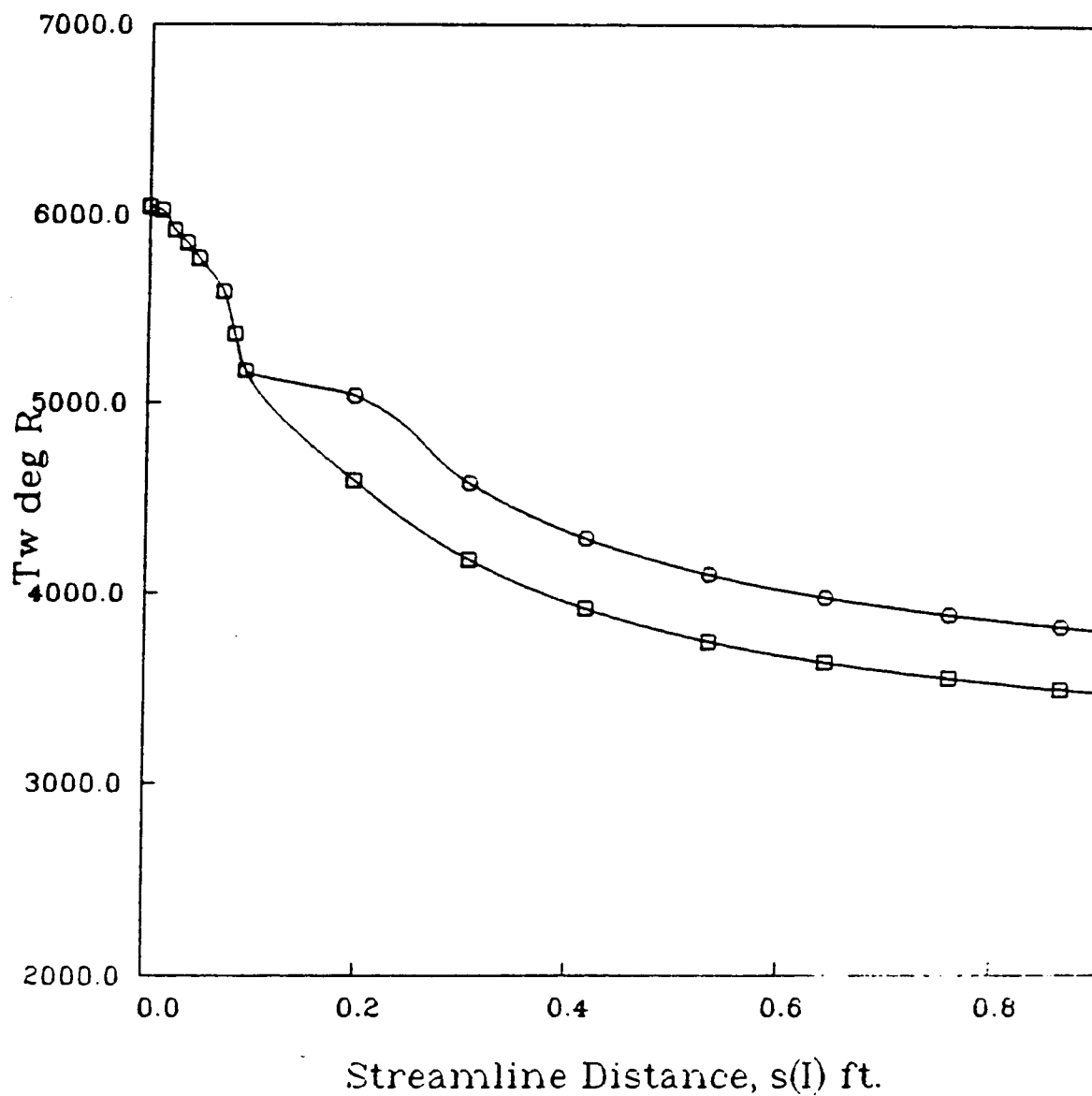


Figure 2

SSTO Surface Heat Flux vs. Wall Mass Injection
Injection of Pure N₂

□ = SSTO/ASCENT-NONCATALYTIC
○ = SSTO/ASCENT-GAMMA=0.0036
△ = SSTO/ASCENT-FULLY CATALYTIC

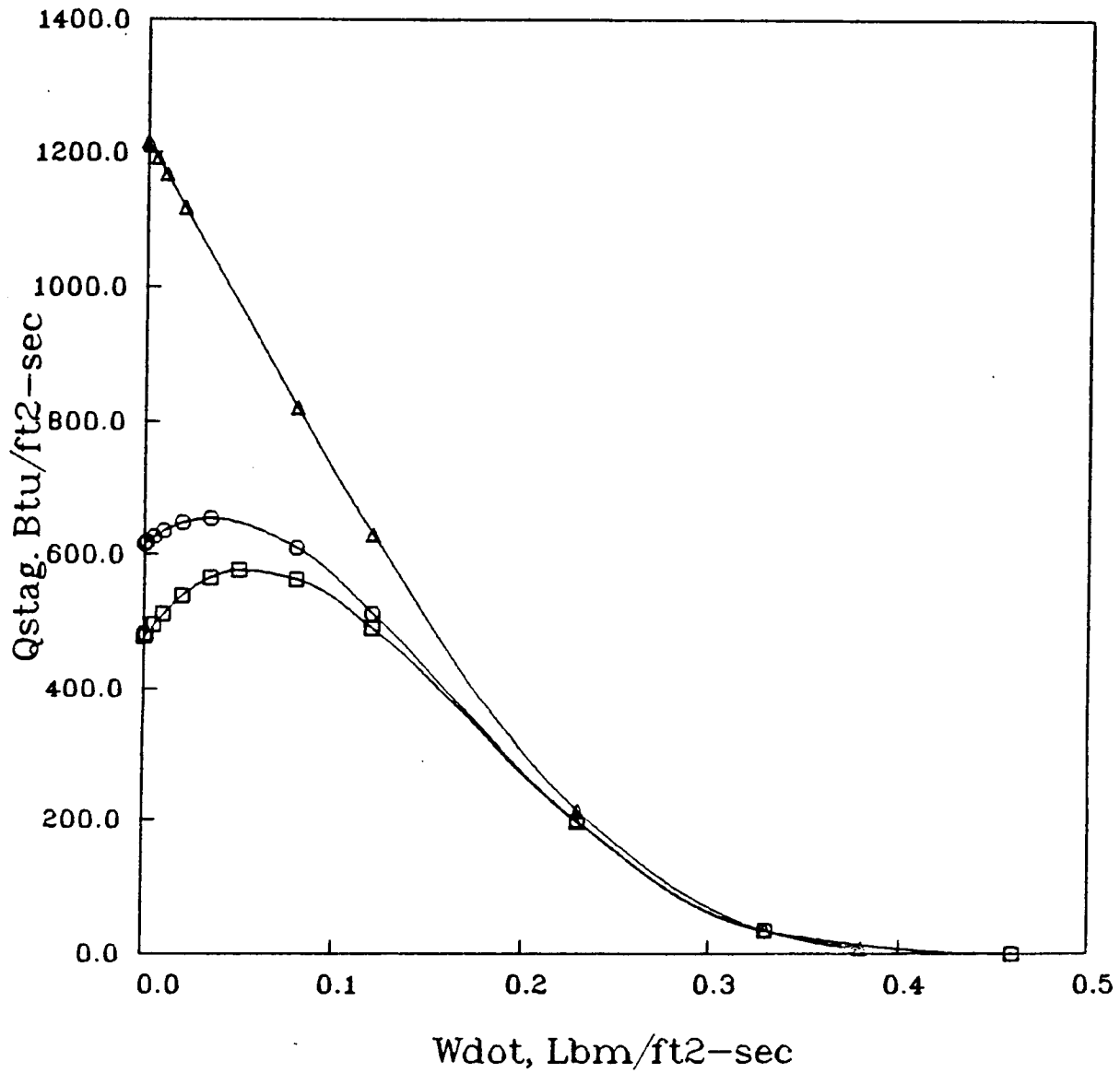


Figure 3

SSTO Surface Heat Flux vs. Wall Mass Injection
Injection of Pure Helium

□ = SSTO/ASCENT-HE/NONCATALYTIC
○ = SSTO/ASCENT-HE/FULLY CATALYTIC

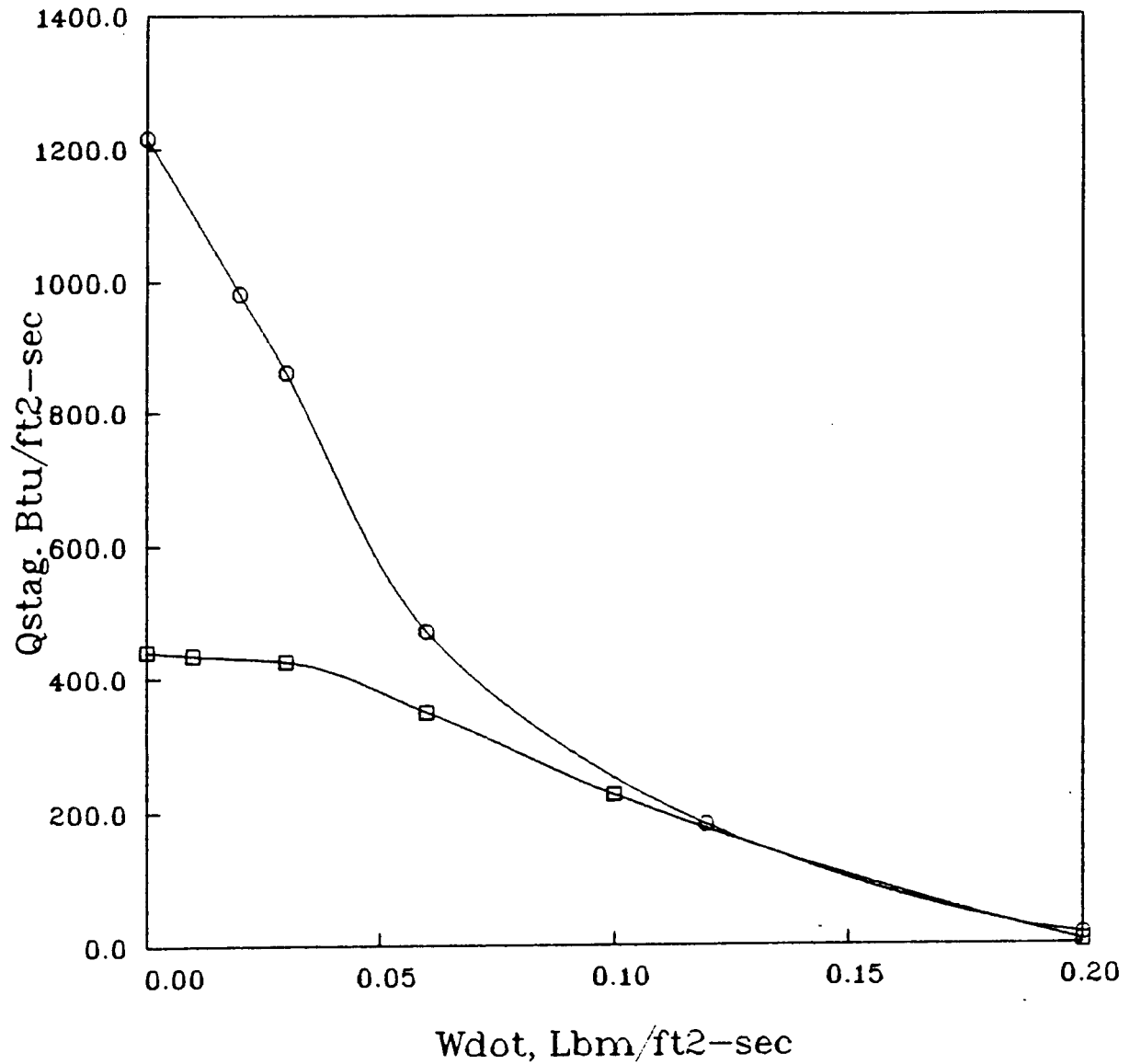


Figure 4

SSTO Surface Heat Flux vs. Wall Mass Injection
Injection of Pure Argon

□ = SSTO/ASCENT-FULLY CATALYTIC
○ = SSTO/ASCENT-NON-CATALYTIC

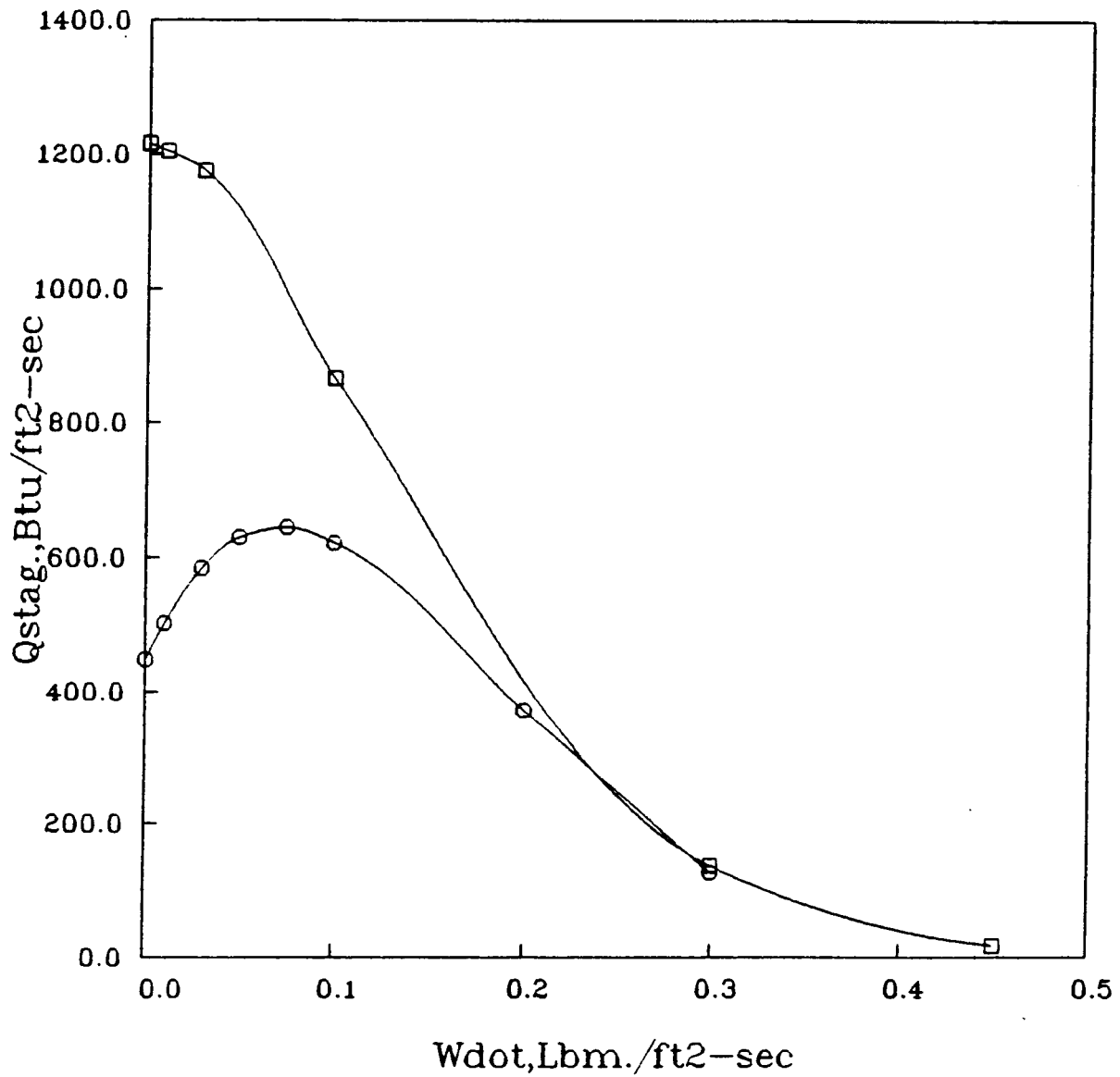


Figure 5

SSTO Surface Heat Flux vs. Wall Mass Injection Comparison of Fully Catalytic Results

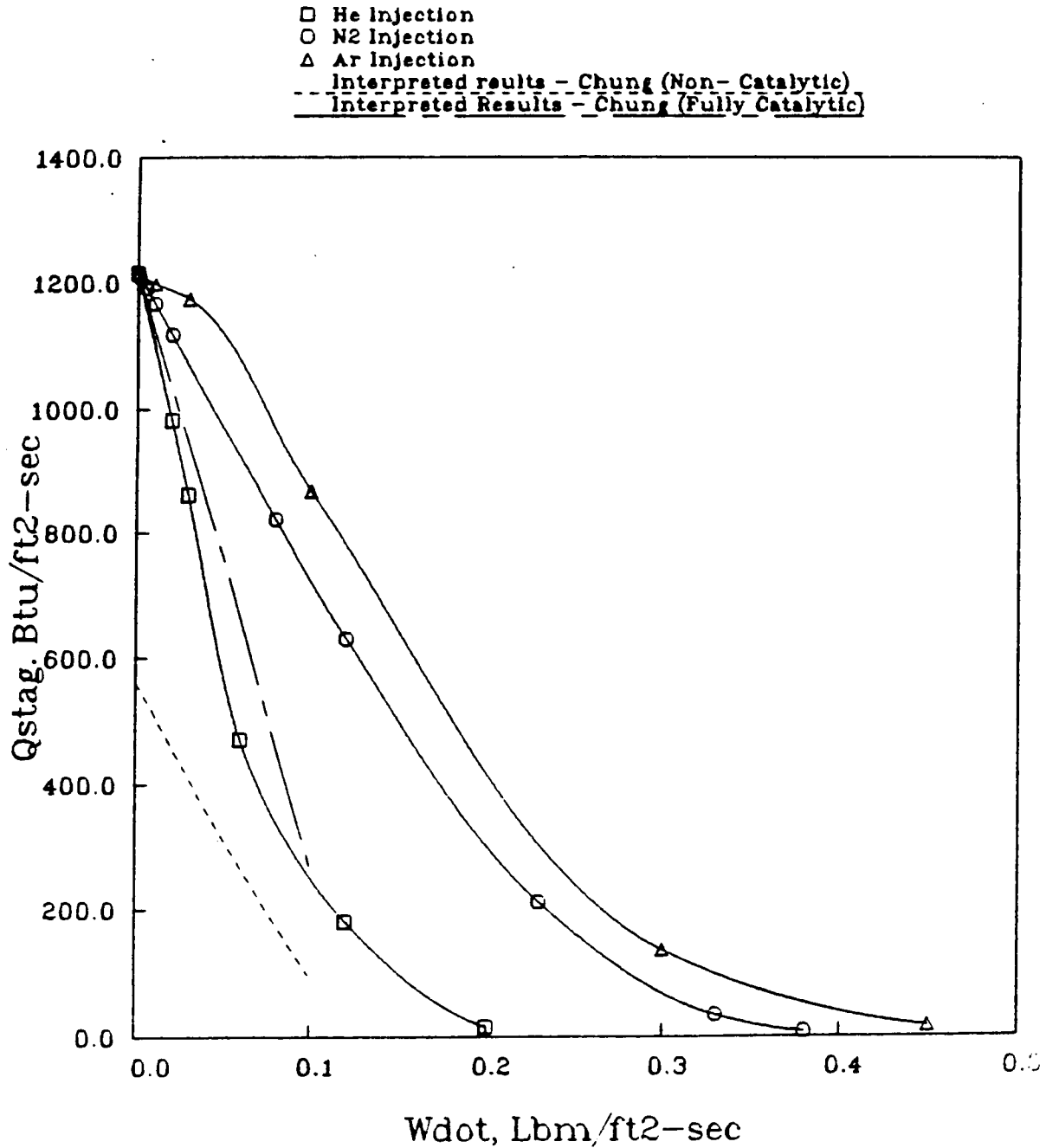


Figure 6

SSTO Stagnation Boundary Layer Species Profiles

Full - Catalytic N2 Injection $\dot{M} = 0.0 \text{ Lb/ft}^2\text{-sec}$

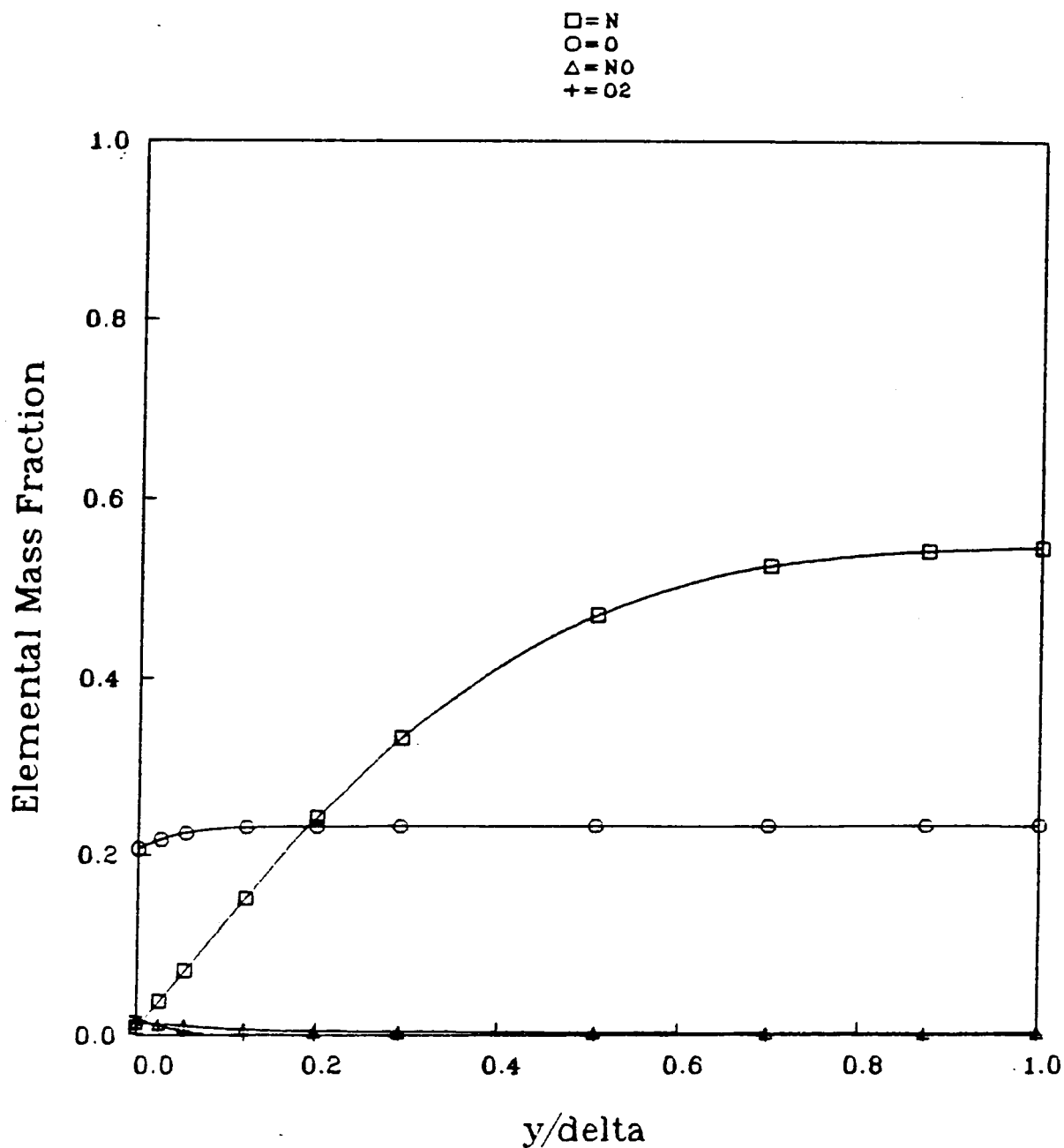


Figure 7

SSTO Stagnation Boundary Layer Species Profiles
Non-Catalytic N₂ Injection $\dot{M} = 0.00 \text{ Lb/ft}^2\text{-sec}$

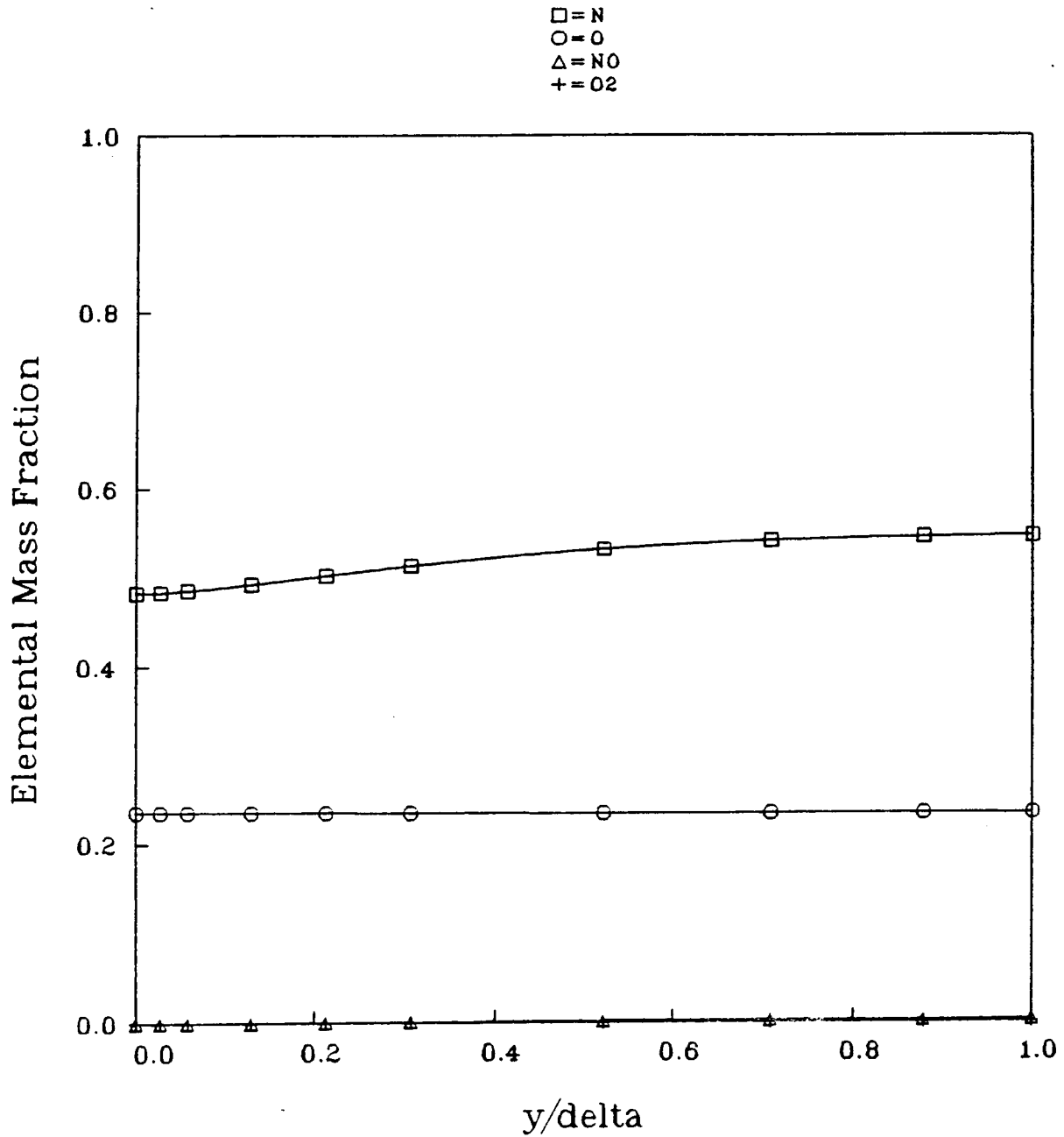


Figure 8

SSTO Stagnation Boundary Layer Species Profiles
Full - Catalytic N₂ Injection $\dot{m}_{\text{dot}} = 0.30 \text{ Lb/ft}^2\text{-sec}$

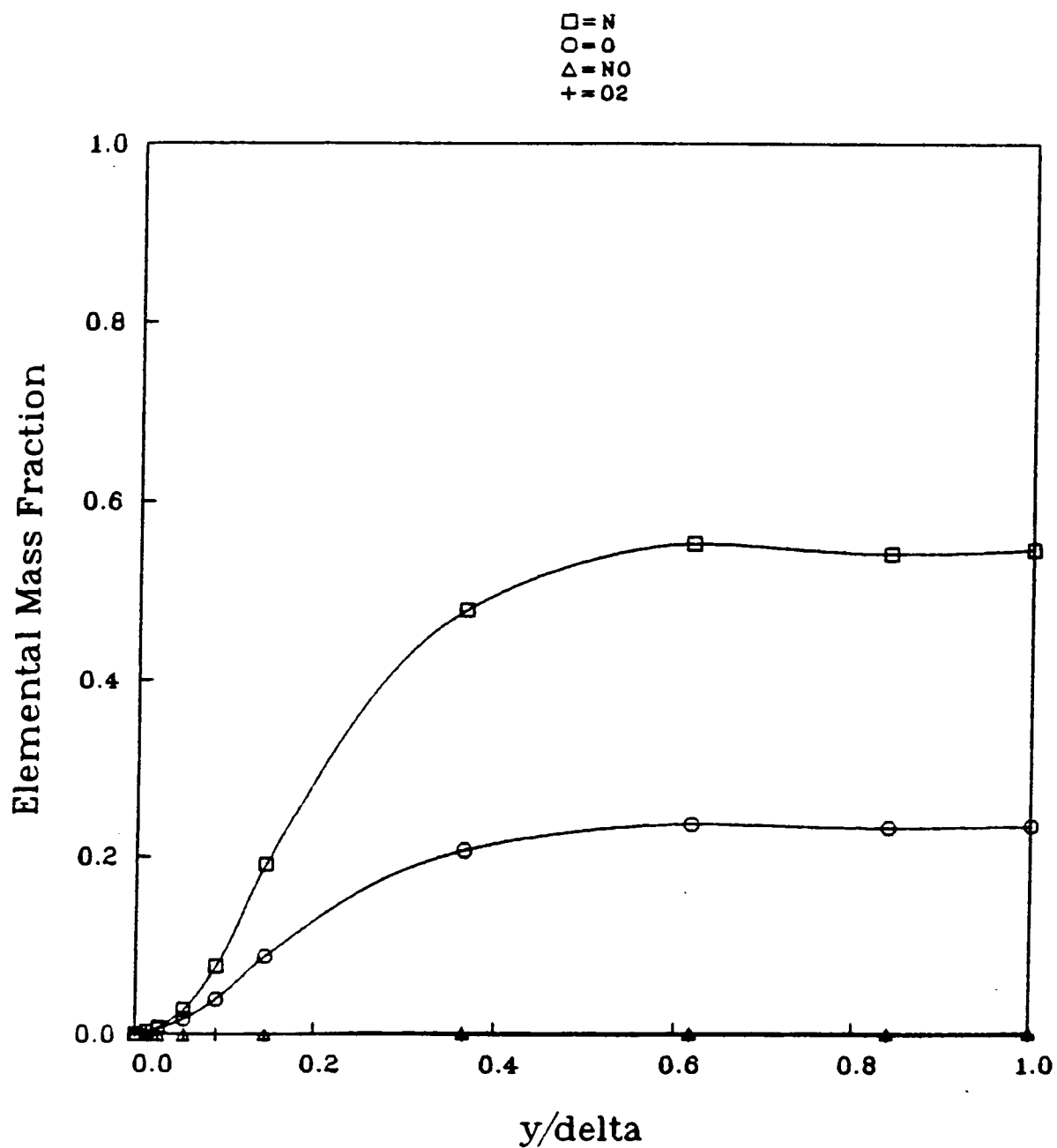
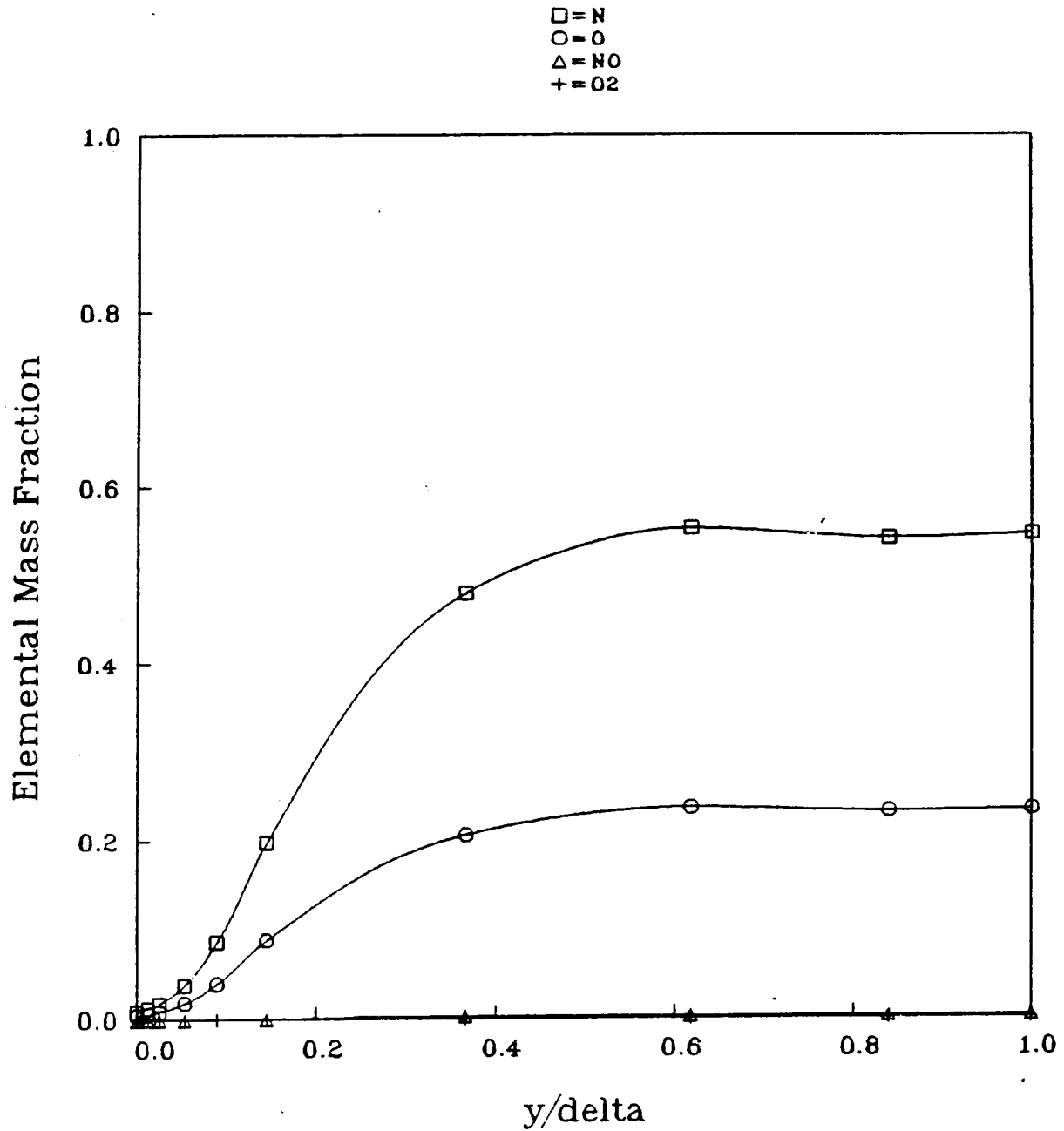


Figure 9

SSTO Stagnation Boundary Layer Species Profiles
Non - Catalytic N₂ Injection $\dot{M} = 0.30 \text{ Lb/ft}^2\text{-sec}$





Report Documentation Page

1. Report No. NASA CR-177516	2. Government Accession No.	3. Recipient's Catalog No.	
4. Title and Subtitle Transpiration Cooling of Hypersonic Blunt Bodies with Finite Rate Surface Reactions		5. Report Date February 1989	
		6. Performing Organization Code	
7. Author(s) William D. Henline		8. Performing Organization Report No. A-89018	
		10. Work Unit No.	
9. Performing Organization Name and Address Sterling Federal Systems, Inc. 1121 San Antonio Road Palo Alto, CA 94303		11. Contract or Grant No. NAS2-11555	
		13. Type of Report and Period Covered Contractor Report	
12. Sponsoring Agency Name and Address NASA Ames Research Center Moffett Field, CA 94035		14. Sponsoring Agency Code	
15. Supplementary Notes Point of Contact: Robert A. Carlson, MS 233-15, Ames Research Center, Moffett Field, CA 94035 (415) 694-6036 or FTS 448-6036			
16. Abstract <p>A study of the convective heat flux blockage to blunt body, hypersonic vehicles by transpiration cooling is presented. A review is given for the general problem of mass addition to laminar boundary layers. Results of similarity analysis of the boundary layer problem are provided for surface heat flux with transpiration cooling. Detailed non-similar results are presented from the numerical program, BLIMPK. Comparisons are made with the similarity theory. The effects of surface catalysis are investigated.</p>			
17. Key Words (Suggested by Author(s)) Transpiration, Mass addition, Surface catalysis, Similarity theory, Boundary layers		18. Distribution Statement Unclassified – Unlimited STAR Category – 34	
19. Security Classif. (of this report) Unclassified	20. Security Classif. (of this page) Unclassified	21. No. of pages 32	22. Price A03